Environmental Science and Pollution Research (2019) 26:30561–30574
https://doi.org/10.1007/s11356-017-1036-5

WATER ENVIRONMENT PROTECTION AND CONTAMINATION TREATMENT

Risk assessment of groundwater environmental contamination: a case study of a karst site for the construction of a fossil power plant

Fuming Liu[1,2,3] · Shuping Yi[1,2] · Haiyi Ma[4] · Junyi Huang[1] · Yukun Tang[4] · Jianbo Qin[4] · Wan-huan Zhou[3]

Received: 16 August 2017 / Accepted: 12 December 2017 / Published online: 20 December 2017
© Springer-Verlag GmbH Germany, part of Springer Nature 2017

Abstract

This paper presents a demonstration of an integrated risk assessment and site investigation for groundwater contamination through a case study, in which the geologic and hydrogeological feature of the site and the blueprint of the fossil power plant (FPP) were closely analyzed. Predictions for groundwater contamination in case of accidents were performed by groundwater modeling system (GMS) and modular three-dimensional multispecies transport model (MT3DMS). Results indicate that the studied site area presents a semi-isolated hydrogeological unit with multiplicity in stratum lithology, the main aquifers at the site are consisted of the filled karst development layer with a thickness between 6.0 and 40.0 m. The poor permeability of the vadose zone at the FPP significantly restricted the infiltration of contaminants through the vadose zone to the subsurface. The limited influence of rarely isotropic porous karstified carbonate rocks on the groundwater flow system premised the simulate scenarios of plume migration. Analysis of the present groundwater chemistry manifested that that the groundwater at the site and the local area are of the HCO_3–Ca, HCO_3, and SO_4–Ca types. A few of the water samples were contaminated by *coliform* bacteria and ammonia nitrogen as a result of the local cultivation. Prediction results indicate that the impact of normal construction and operation processes on the groundwater environment is negligible. However, groundwater may be partly contaminated within a certain period in the area of leakage from the diesel tanks, the industrial wastewater pool, and the cooling tower water tank in case of accidents. On a positive note, none of the plumes would reach the local sensitive areas for groundwater using. Finally, an anti-seepage scheme and a monitoring program are proposed to safeguard the groundwater protection. The integrated method of the site investigation and risk assessment used in this case study can facilitate the protection of groundwater for the construction of large-scale industrial project.

Keywords Groundwater contamination · Integrated site investigation · Risk assessment · Solute transport · Karst hydrogeology

Introduction

Globally, groundwater is vital and a potentially vulnerable water resource for meeting the various water demands in the socioeconomic development, as well as for maintaining a wide diversity of ecosystem functions and services. However, a variety of organic contaminants, anions, metallic ion, and emerging groundwater contaminants (EGCs) derived from diverse municipal, agricultural, and industrial sources and pathways have seriously limited drinking water availability and posed threats to the subsurface microbial ecological systems (Stuart et al. 2012). For instance, the overused and nontarget pesticides used in agriculture are one of the representative non-point pollution sources that have been detected in groundwater widely (Arias-Estévez et al. 2008). Their environment residues in groundwater are notoriously persistent organic contaminants that have been identified as the cause of fish kills, reproductive failure in birds, and illness in humans (Fernández-Cruz et al. 2017).

The rising public concerns on environment and groundwater contamination has caught the attention of governments and scholars. Some progress in groundwater protection has been

Responsible editor: Philippe Garrigues

✉ Shuping Yi
yisp@sustc.edu.cn

[1] Shenzhen Key Laboratory of Soil and Groundwater Pollution Control, Shenzhen, China

[2] School of Environmental Science and Engineering, Southern University of Science and Technology, Shenzhen, China

[3] Department of Civil and Environmental Engineering, Faculty of Science and Technology, University of Macau, Macau, China

[4] Guangdong Electric Power Design Institute, China Energy Engineering Group Co., Ltd., Guangzhou, China

achieved in China via legislation, standardization, and financial support from government and agencies (Li et al. 2017). However, risk assessment of groundwater contamination is still a challenge due to the requirements of multidisciplinary data and limited poor understanding of the site. It has been reported that the intertwined processes of groundwater flow and contaminant transport proceed in three spatial dimensions, in inherently heterogeneous and anisotropic geological media, over a great range of distances and times, and is typically nonstationary (Wachniew et al. 2016; Yi et al. 2012b). Therefore, a solid understanding of the method for obtaining data, full analysis, and application of fundamental data in hydrogeology, geochemistry, environmental engineering, and modeling as well, is crucial for an effective risk assessment of groundwater (Yi et al. 2011). Contamination risks of groundwater include the inherent vulnerability of an aquifer, called static factor, and involve considering anthropogenic activities as significant dynamic factors (Ducci et al. 2008). Moreover, groundwater quality patterns, groundwater pollution quantification, and the risk assessment of groundwater contamination require specialized modeling tools to predict the water flow, dissolved species, and their complex interactions with solid and gaseous phases, such as CORE2D code (Dai and Samper 2004; Samper et al. 2012).

Karst environments are characterized by distinctive landforms and a peculiar hydrologic behavior occurring in around 20% of the emerged Earth's surface and provide approximately 20–25% of the world's drinking water (Parise et al. 2015a). Karst aquifers are well-known for their vulnerability to contamination, especially in large-scale industrial construction, such as P-xylene (PX) chemical industry, nuclear power station, sanitary landfill, disposal of low- and intermediate-level radioactive wastes, or fossil power plant (FPP) (Ford 2007). Vulnerability of karst aquifer systems are mainly from the frequent interaction between surface water and groundwater, intense hydrological dynamic variability, spatially heterogeneous distribution of groundwater, and low depuration capability. Gutiérrez et al. (2014) highlighted that environmental impacts and hazards associated with karst have led to an escalation of karst-related environmental and engineering problems such as sinkholes, floods, and landslides. Consequently, planning engineering works in karst environments should consider such peculiarities and potential risk and take measures to reduce as much as possible the negative impacts on ecosystems, with particular regard to pollution events.

Furthermore, there is often a negative attitude among the society toward risks of a large-scale industrial construction because it is considered as a threat of damage, danger, and of other potential side effects (Shan and Zhang 2012). An effective risk assessment and prediction of groundwater environmental contamination prior to construction renders enormous help as it provides valuable suggestions for the management of the project operation and groundwater pollution prevention and control, and more importantly, convinces the public. China is one of the richest countries in the world that has construction projects in peculiarities karst environment. Nevertheless, there is limited literatures reporting the risk assessment of groundwater in karst environment induced by a large-scale industrial construction.

In this paper, an integrated approach is used for the risk assessment of groundwater contamination based on the construction of an FPP at a karst and shale site. The studied FPP is a power station to be constructed which burns coal to produce electricity and use light diesel oil as the ignition oil. A series of on-site investigations of boreholes, geophysical prospecting, field tests, and laboratory analysis were conducted to obtain fundamental data regarding the hydrogeological characteristics of the site. Furthermore, the transports of contaminants from different sources of pollution were numerically modeled and predicted by groundwater modeling system (GMS) equipped with modular three-dimensional multispecies transport model (MT3DMS) code. Finally, environmental anti-seepage and monitoring programs were proposed for the construction and operation of the FPP and its affiliated ashery (dry fly ash landfill) aiming to reduce the negative impacts on ecosystems.

Site background

The study site is located on the eastern bank of the Beijiang River, Guangdong province, China (Fig. 1). The FPP and its affiliated ashery (namely the dry fly ash landfill) are at a distance of about 2 and 2.5 km to the east of the Beijiang River, respectively. The installed capacity of the FPP is 2×1000 MW, with the compensation water of 3300 m^3/h (namely 0.917 m^3/s). Information from the feasibility report for the project revealed that the annual weights of coal ash and slag generated by the FPP are 6.95×10^5 and 1.3×10^5 tons, respectively. After compression control, the annual volumes of produced coal ash and slag can be reduced to approximately 6.6×10^5 m^3. This could be a potential pollution source for the FPP in the event of an accident.

The study site extends over an area of 35 km^2 with the FPP and the ashery as its center. The elevation of the site ranges from 45 to 80 m above sea level (asl). Low hills are situated to the north, east, and south of the site. The hills located to the south and east sides of the site are dominated by carbonate rock terrigenous formations that give rise to part of the classical karst topography, with relatively steep slopes at an elevation of 100–204 m asl. The hills located to the north site are composed of mudstone, at an elevation of around 60–86 m asl. West of the site is a basin with geological stratum constituted of gravel and silty clay, and shale bedrock is present. There are several villages and industrial plants in the basin. Part of the groundwater is pumped for local drinking and irrigation, and

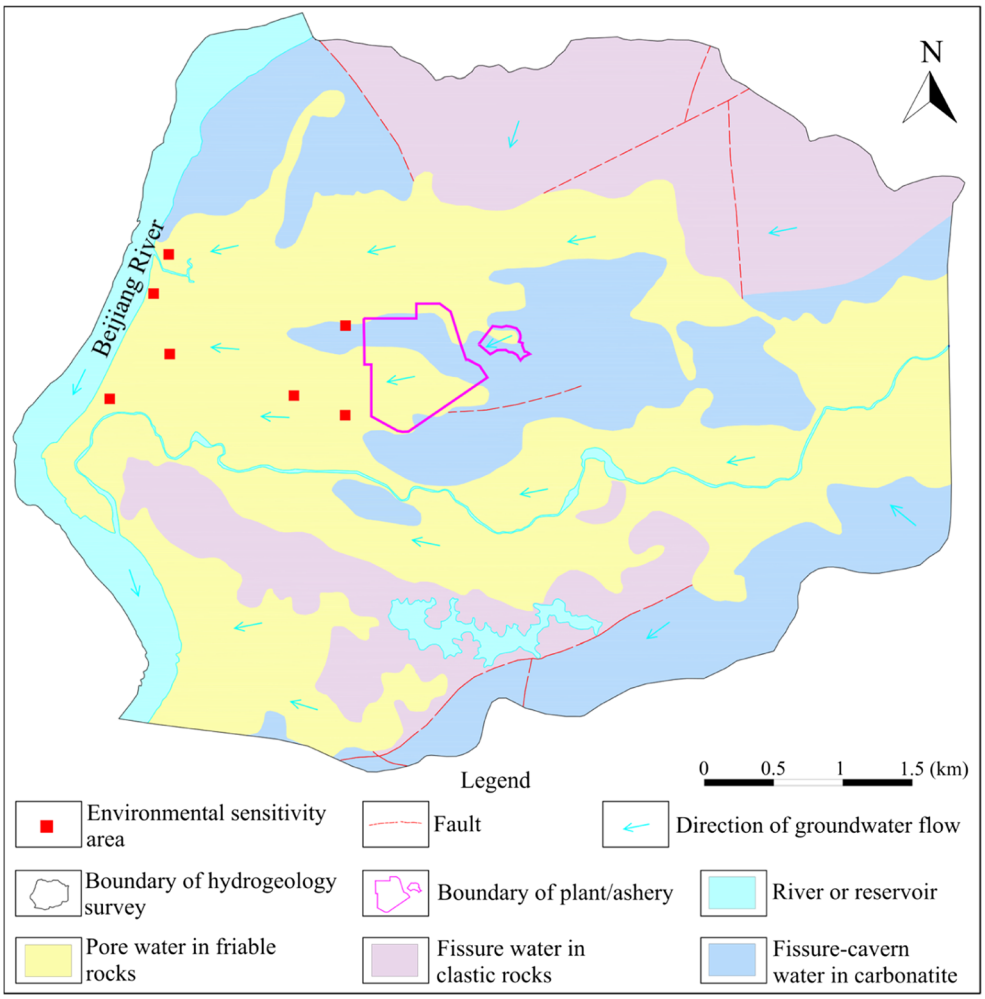

Fig. 1 Location of the study area and the hydrogeological characteristics of the site

the groundwater discharges to the Beijiang River, offering as water source for local cities. Therefore, it is necessary to understand the groundwater properties, and a detailed risk assessment should be performed to evaluate the possibility of groundwater contamination prior to the design and construction of the FPP and the ashery in the site area.

Assessment program

Integrated on-site program

The risk of groundwater is from interaction between the vulnerability of aquifers and contamination due to anthropogenic activities. Feasibility of the risk assessment of groundwater environmental contamination includes three factors: (1) suitable method that can be applied to obtain the specific data of the intrinsic vulnerability of the vadose zone and the aquifer, (2) effective prediction of contaminant hazards released from the pollution sources, and (3) reliable suggestions for environmental measures to prevent groundwater from being polluted (Calò and Parise 2009; Zhang et al. 2016).

In order to achieve the requirements for the groundwater risk assessment for the FPP and the ashery, a systematic approach was proposed for the risk assessment of groundwater environmental contamination, as shown in Fig. 2. Firstly, a complete review was conducted including the regional hydrogeologic and engineering geological investigation and engineering project feasibility studies of the FPP and ashery. A surface surveying regional hydrogeological survey at a scale ratio of 1:10,000 was first performed to examine the main geological and hydrogeological characteristics of the site. Secondly, a detailed investigation of the pollution sources and monitoring was carried out to collect the information of local sensitive areas as well as the current environmental conditions. Consequently, the classification of the sensitive areas can be confirmed base on their vulnerabilities. Thirdly, hydrogeolocical drilling, hydrogeological tests, and geophysical prospecting were implemented aiming to collect the detailed hydrogeology data, especially for karst. Simultaneously, groundwater was sampled and analyzed during hydrogeological drilling and tests. All samples collected for laboratory analysis were proceeded without disturbance during sampling and delivery. The solute dispersion properties

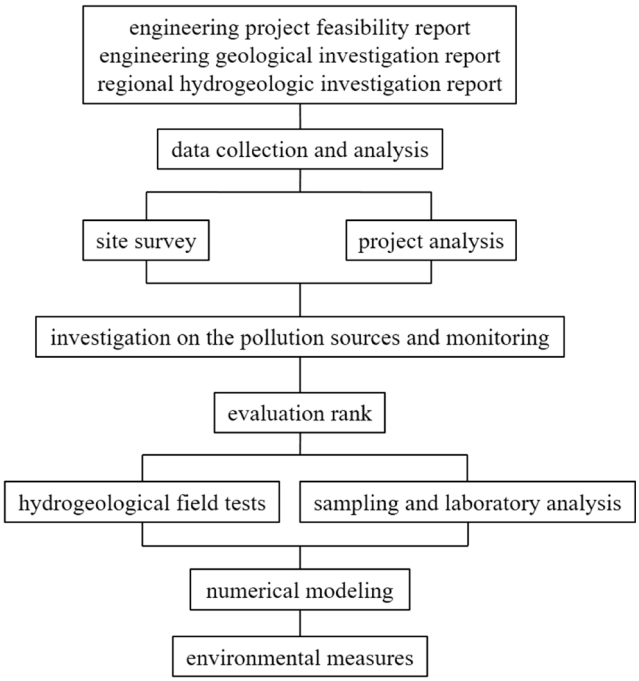

Fig. 2 Integrated approaches for the risk assessment of groundwater environmental contamination for the construction of the FPP and ashery

were determined by an on-site dispersion experiment with NaCl injection in one borehole and measured in the observation borehole. The Standmod program was used to calibrate the variation of Na^+ concentration and to estimate the dispersion coefficient (Feinstein and Guo 2004). Finally, based on the specific data obtained from hydrogeological tests, the groundwater flow and solute transport models were applied to evaluate the contamination risk of the FPP and ashery in the ambient groundwater environment (Yeh 2015).

Evaluation ranking for the groundwater environment

Risk assessment of groundwater determines the qualitative analysis of risk potential regarding the sensitivity or vulnerability of the subsurface environment. Therefore, confirmation of the evaluation ranking for the groundwater environment is the prerequisite for risk assessment. In order to classify the groundwater environmental vulnerability, improve the efficiency and precision of an assessment, and to meet the requirement of relative regulations, the ranking of groundwater environmental factors was evaluated in this study case according to *Technical Guidelines for Environmental Impact Assessment of Groundwater Environment* (HJ610–2016).

The assessment classification of groundwater environmental vulnerability is shown in Table 1. Several groundwater environmental factors, including the capability of self-purification in the vadose zone, the vulnerability of the aquifer, the sensitivity of the groundwater environment, the intensity of sewage discharge, and the complexity of sewage content, are considered (Anand et al. 2016). As no distinctive feature of groundwater environmental vulnerability was found, the evaluation rank of the groundwater environmental vulnerability for the site of the FPP and the ashery is assigned to the secondary class based on *Technical Guidelines for Environmental Impact Assessment of Groundwater Environment* (HJ610–2016), specifying the content and depth of the on-site investigations, experiments, and analysis of the karst hydrogeological condition of the site.

Evaluation factor and protection target

Groundwater pollution may involuntarily or accidentally happen in the construction and operation period of the FPP. During the engineering project construction period, the main potential pollution sources of groundwater are dominated by domestic sewage and contingent leakage of fuel oil from the engines. Consequently, contaminants of COD_{Mn}, NH_3–N, suspended solids (SS), and petroleum oil are the main contaminants in the groundwater environment evaluation. While during the operating period, sulfate, chloride, and petroleum oil contribute to the main factors of the groundwater environmental evaluation, given the point sources of the diesel tank (DT), the industrial wastewater pool (IWP), and the cooling tower water tank (CTWT). For the monitoring factors of the groundwater environment, the pH, water hardness, SO_4^{2-}, Cl^-, F^-, NO_2^-, NO_3^-, Fe^{2+}, Fe^{3+}, Mn^{2+}, Hg^{2+}, As^{3+}, Cd^{2+}, Pb^{2+}, Cr^{6+}, COD_{Mn}, NH_3–N, volatile phenol, petroleum oil, and fecal coliform in the groundwater are parameters for the evaluation.

Protection of sensitive groundwater areas is the motivation that promotes the progress of risk assessment of groundwater contamination. In this study case, seven sensitive groundwater areas located in the vicinity of the FPP and the ashery were inspected and confirmed (Fig. 1). Since part of the groundwater for washing and irrigation is supplied from decentralized domestic wells in the basin area where the investigated site is located, simultaneously considering the possibility of emergency water supplies, seven decentralized domestic well areas are confirmed as environmentally sensitive areas except for the Beijiang River downstream of the FPP, to the west of the site. Thus, these seven decentralized domestic wells were confirmed as the environmental protection objectives for this risk assessment.

Result and discussion

Karst development

A quantitative understanding of the hydrogeological characteristics of the site is essential for groundwater assessment for the engineering project. The studied site lies in the south of Dadong mountain-Guidong east-west tectonic zone, and the north of Renhua-Yingde-Sanshui Cathaysian drape tectonic

Table 1 The evaluation rank of the groundwater environment for the risk assessment of the FPP and the ashery

Position/item	Overall	Capability of self-purification in vadose zone	Vulnerability of pollution in aquifer	Sensitivity of groundwater environment	Intensity of sewage discharge	Complexity of sewage content
FPP	Secondary	Medium	Medium	Sensitive	Minor	Medium
Ashery	Secondary	Medium	Medium	Sensitive	Minor	Medium

zone. The tectonic zone at the site comprise quaternary bed, Devonian mudstone, marlstone and limestone, no other time-stratigraphic appeared.

Both the FPP and its affiliated ashery are seated in a synclinal basin where karst developed. The ashery is located to the east of the FPP. Erosion-deposition type and corrosion type dominate the basic geomorphology of the basin. Erosion-deposition type geomorphology distributes in strip-type, constituted of diluvium quaternary system, while the corrosion type geomorphology characterizes the hills, composed of thick Devonian limestone. Similar to the regional hydrogeology, quaternary, Devonian, carboniferous and Cambrian rocks domain the site lithology. For the quaternary strata, they are developed from the terrace deposit at the Beijiang River. Its substrate consists of grait, gravelly sand, and conglomeratic silty clay. Carboniferous strata restrictively appear in the west-south of the FPP, fine-crystalline dolomite, micrite, and dolomite are the prime matrices. Cambrian strata are metamorphic and slightly spread around FPP, with medium-fine quartz sandstone, feldspar-quartz sandstone, and silk mica slate as the main content. Unlike Cambrian strata, Devonian strata are widely distributed around the site, exhibiting the north-east trend.

Karst is a distinctive terrain developed on the soluble rock with landforms related to various underground drainage condition that can be very difficult ground for civil engineers as they threaten foundation integrity (Waltham and Fookes 2011). In this case study, a comprehensive analysis of the characteristics has been performed for the karst development of the site. The parameters of the karst ratio (K_v), the planar karst ratio (K_p), and the average linear karst ratio (K_l) calculated from the on-site geophysical prospecting, as well as the boreholes distributed evenly throughout the site have been used to indicate the spatial karst development:

$$K_V = \frac{V_k}{V_t} \times 100\% \quad (1)$$

$$K_p = \frac{A_k}{A_t} \times 100\% \quad (2)$$

$$K_l = \frac{\sum L_k}{\sum L_t} \times 100\% \quad (3)$$

where V_k is the volume of the estimated karstified carbonates in the investigated site; V_t is the total volume of the investigated site; A_k is the amount of the borehole in which karstified carbonates is found; A_t is the total quantity of the borehole; L_k is the length of the karstified carbonates in a borehole; and L_t is the total length of a borehole.

A classification of karst on the site based on their karst characteristics was proposed according to the *Code for geotechnical investigation of fossil fuel power plant* (GB 51031–2014). Basically, the karst development on the site can be divided into three sub-zones, namely very strongly developed zone (I), strongly developed zone (II), and intermediate-slightly developed zone (III), as shown in Fig. 3. The very strongly developed zone (I) traverses the site. It exhibits an area of very strong karst development. Dozens of karst caves have been disclosed by the boreholes with a K_v value up to 37.36%. Most of the caves are less than 0.4 m in height, a karst cave with the maximum height of 11.0 m was identified. The karst caves are mainly developed at the middle-south of the basin where the carbonate rock layer is thick. It has been found that the K_p and K_l are 71.5 and 26.22%, respectively, with an average depth of 17.0 m below the surface.

In the strongly developed zone (II) located in the south and middle of the basin, karst caves are generally found near the surface. The karst caves were mainly disclosed at a depth ranging from 16.0 to 30.0 m for the sub-zone in the north of the basin. For these two sub-zones (II) located in the south and middle of the basin, the calculated K_v and K_l are 26.3 and 11.5%, respectively.

In contrast, only three karst caves were disclosed at the most northern area of the basin, with the K_v and K_l only about 15 and 4.2%, respectively. Correspondingly, karst has been determined as an intermediate-slightly developed zone (III) (Marín et al. 2010). Karst presents a complex medium with multi-scale heterogeneity on this site. However, no shallow buried river, hall- or corridor-type karst caves were developed at the site nor large-scale well-connectivity karst channels. Due to the fact that almost all the karstified carbonates framework in the three regions were filled with silt clay during the hydrogeological drilling, the three karst hydrosystems presented relative low permeability resulting in slow movement of groundwater through silt clay filled karst conduits and retardative pressure transfer occurrences (Worthington et al. 2001).

Characteristics of vadose zone

The vadose zone plays a vital role in retarding the migration of solutes (Khaleel 2007); therefore, characterization of the

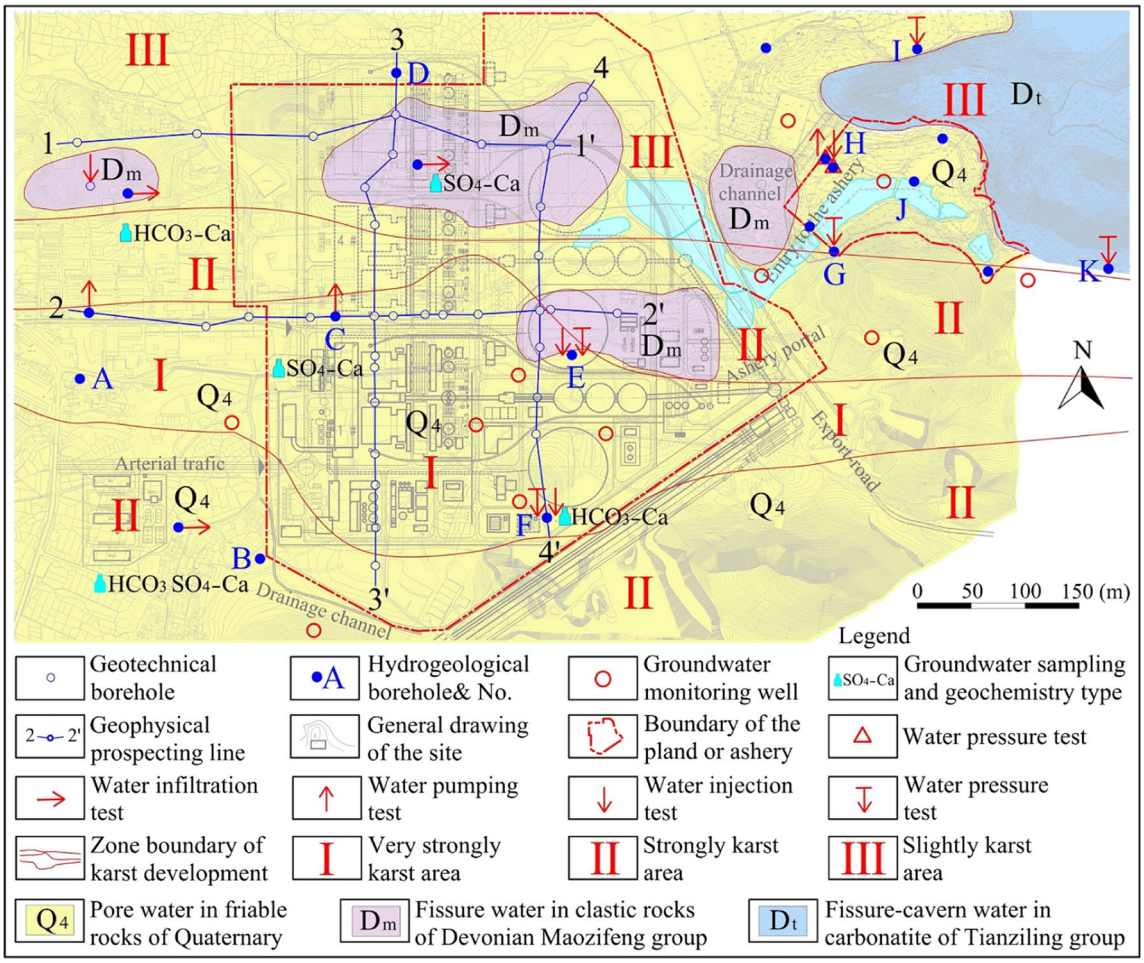

Fig. 3 On-site field work and distribution of karst development around the site

vadose zone is crucial for a field assessment program (Li et al. 2015). The vadose zone of the site where the FPP and the ashery are located is dominated by quaternary deposits, and only a small amount of Devonian mudstone and limestone is scattered at the south and north of the FPP, as well as at the slope region bounding the ashery. The contour map of the vadose zone thickness is derived from boreholes and is shown in Fig. 4. The results show that the thickness of the vadose zone is about 2 to 6 m in the east-south part of the FPP, constituted of weathered limestone. The thickness of the vadose zone in the central part of the FPP varies between 2.0 and 8.0 m, composed of artificial fills, muddy soil, and alluvial clay. The vadose zone in the northern FPP is thicker than that of central and southern part, with thickness between 8.0 and 20.0 m. The lithology of this part of the vadose zone is governed by a thin layer of mudstone, silty mudstone, and marl along with partial argillaceous siltstone.

The permeability of the vadose zone at the FPP is poor to an average vertical hydraulic conductivity value of 3.40×10^{-5} cm/s obtained from water injection tests in pit experiments. The vadose zone acts as a horizontal cutoff wall with a favorable parameter that can significantly restrict the infiltration of contaminants through the vadose zone to the subsurface (Goss et al. 2010).

Aquifers and aquitards

Phreatic aquifers act as a principal lens for contaminants in view of storage, interaction, and migration (Gurdak and Qi 2012). The results indicate that the aquifers were mainly constituted of pore water in friable quaternary rocks, fissure-cavern water in carbonatite, and fissure water in clastic rocks. Pore water in friable quaternary rocks is widely distributed on the site, with several discrete patches, constituted of fissure-cavern water in carbonatite and fissure water in clastic rocks. A typical vertical distribution of aquifers at the FPP is shown in Fig. 5. The result reveals that intensely karstic development was verified in the aquifer where fissure-cavern water in carbonatite is covered, with the K_p and K_l of 71.5 and 26.22%, respectively. The aquifers consist of the filled karst development area with a thickness between 6.0 and 40.0 m, mainly distributed in the central-southern part of the site. The embedded depth of the groundwater level varies from 0.2 to 10.0 m. Groundwater levels show seasonal variation, and

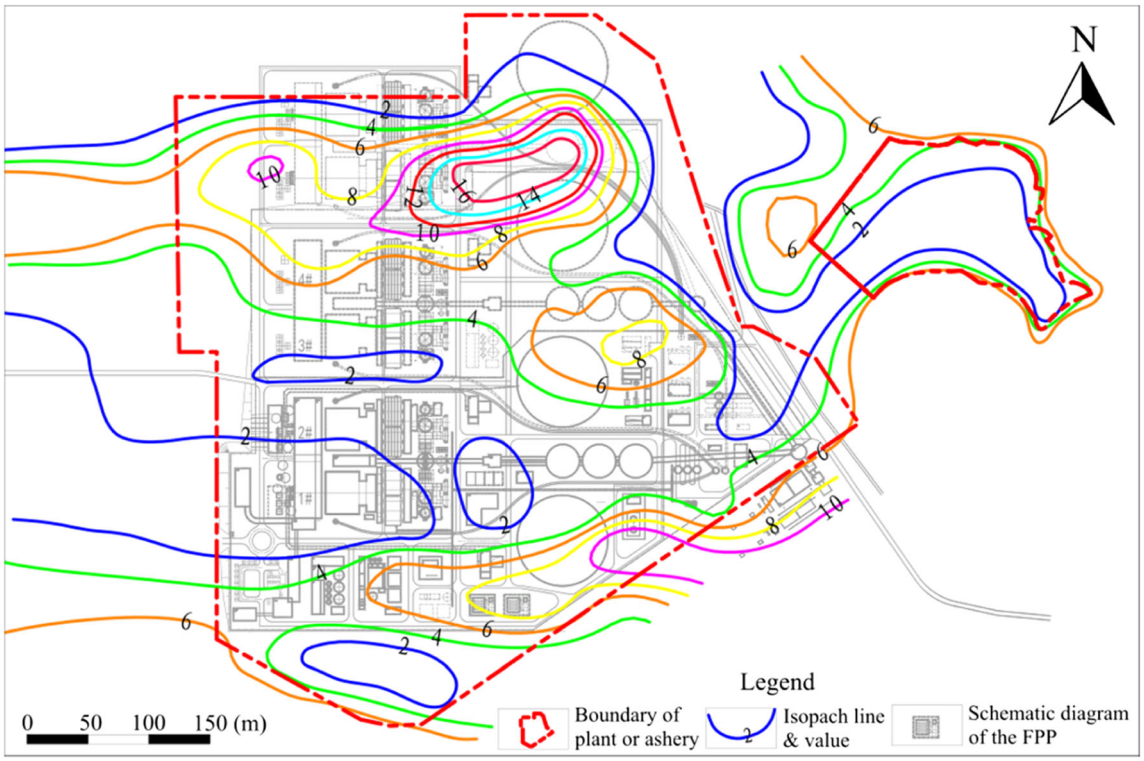

Fig. 4 The contour map of the thickness of the vadose zone

atmospheric precipitation is the primary supply of phreatic aquifers. To some extent, the silt clay filled karst hydrosystems provide a buffer effect on the phreatic water level. The average annual precipitation in this region is 1881 mm and the evaporation is 1635 mm (data collected for years from 1959 to 2015). The rainy season commences in April and ends in September with the heaviest precipitation between April and June. The thickness of the aquifers is relatively thin and coupled with the fact that the water volume is small, it does not serve as the main source of water supply for FPP.

In situ batch drilling pumping testing, water pressure testing, and double orifice dispersion testing were performed per the site-specific conditions for each test. Parameters were estimated independently with equations appropriate to the test methods (Mayer et al. 2002; Zech et al. 2015). The pumping test was conducted at both the site of the FPP and ashery in triplicate at each drilling

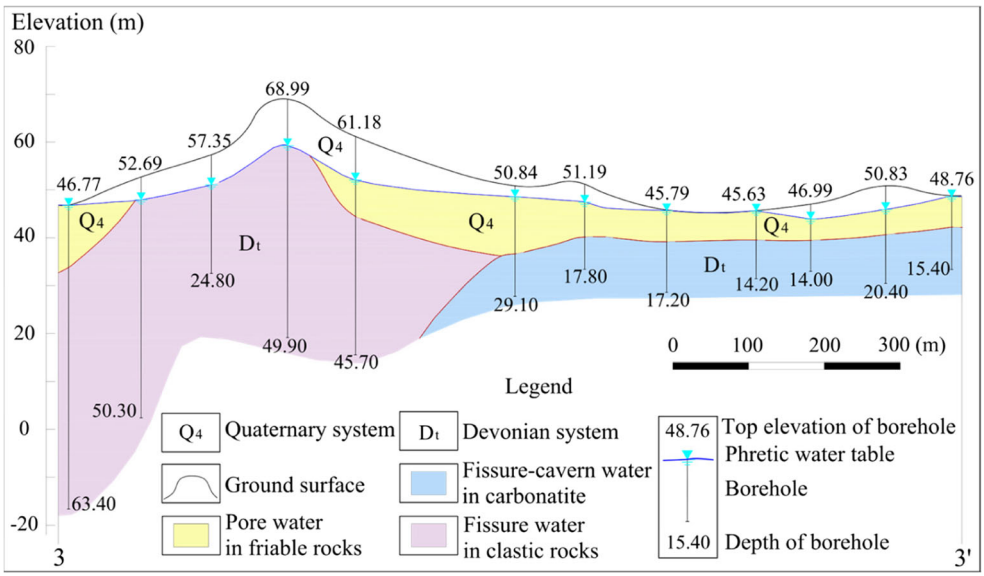

Fig. 5 A north-south hydrogeological cross-section of the site (3–3′ section shown in Fig. 3)

Table 2 Result of the pumping test at the aquifers

Position	Order	Volume of water inflow Q (L/min)	Drawdown of pumping water S (m)	Thickness of aquifer h (m)	Diameter of pumping hole r (m)	Radius of influence R (m)	Permeability cm/s	Average value (cm/s)	Classification of permeability
FPP	1st time	5.03	1.31	18.3	0.054	6.94	3.25×10^{-4}	3.20×10^{-4}	Medium permeable
	2nd time	9.25	2.61	18.3	0.054	14.08	3.37×10^{-4}		
	3rd time	13.53	4.81	18.3	0.054	24.03	2.90×10^{-4}		
Ashery	1st time	3.59	2.50	11.20	0.054	6.98	2.02×10^{-4}	1.80×10^{-4}	Medium permeable
	2nd time	4.54	3.70	11.20	0.054	9.80	1.81×10^{-4}		
	3rd time	5.00	5.40	11.20	0.054	13.41	1.59×10^{-4}		

hole (Fig. 3). The permeabilities of the aquifer in the FPP and ashery are stable at 3.20×10^{-4} and 1.80×10^{-4} cm/s, respectively (Table 2). Water pressure tests were used to estimate the hydraulic conductivities for the slightly weathered limestone (Chandra et al. 2016; Lacey 2016) and the results are listed in Table 3. All the P-Q curves of the water pressure tests are classified as either C or E type, namely the 1 Lu regarded as 10^{-5} cm/s to approximate the permeability value (Mejías et al. 2009). The average permeability value of the slightly weathered limestone is estimated at about 1.20×10^{-5} cm/s, which can regard as the aquitard below the aquifers. From Tables 2, 3, and 4, the results demonstrate that there is a tiny difference among the permeability values around the site, yet they are found to be scale-dependent and almost in the same order of magnitudes.

Figure 6 shows the comparison between the measured and the modeled concentrations of Na^+. Results indicate that the groundwater flow rate of 0.0215 m/h, with a longitudinal dispersity, α_L, and a transverse dispersity, α_T, equal to 0.033 and 0.009 m, respectively. The calibrated value of hydraulic conductivity is 1.57×10^{-4} cm/s for the data from the dispersion experiment, consistent with the values that from the pumping test (Table 4).

Groundwater flow

A precise description of groundwater flow is one of the essential elements for an effective risk assessment of groundwater and for the analysis of migration of contaminants (Pfunt et al. 2016). Groundwater flows generally in the direction from east to west and the Beijiang River and its tributaries are the fundamental receivers of groundwater (Fig. 7). The shallow groundwater in this study case is mainly recharged by precipitation and lateral flows from the eastern and southern boundary areas. Part of recharges are from the Beijiang River during the rainy season. Evapotranspiration is extensive in the valley areas and the scattered domestic wells offer additional discharge of groundwater in the area. The studied site presents a semi-isolated hydrogeological unit with groundwater discharge to the Beijiang River along the western boundary. On the other hand, the contour map of the measured water table via drilling indicates that the water table in this site is unified and continuous. Based on the analyses of regional field tests and water table monitoring, conclusion could be drawn that the karstified carbonates, clastic rocks, and friable rocks framework, in which very strongly developed zone, strongly developed zone, and intermediate-slightly developed zone included, is hydraulically continuous, which premised the correct interpretation and modeling of solute transport (Kaufmann and Braun 1999).

Present groundwater chemistry

The concentrations of major and minor ions of groundwater are essential in understanding anthropogenic and geochemical processes affecting water quality (Idris et al.

Table 3 Result of the water pressure test in boreholes at the aquitards

Lithology	Borehole no.*	Position	Depth (m)	Permeable rate (Lu)	Permeability (cm/s)	P-Q curve	Average value (cm/s)	Classification
Lightly weathered limestone	E	FPP	12.9~17.8	2.32	8.36×10^{-6}	C type	1.20×10^{-5}	Aquitard
	F	FPP	15.4~19.5	2.22	2.65×10^{-5}	E type		
	G	Ashery	14.7~19.1	0.94	1.14×10^{-5}	F type		
	H	Ashery	15.1~19.9	0.49	6.05×10^{-6}	C type		
	K	Ashery	26.2~32.5	0.66	8.69×10^{-6}	E type		

* The borehole position is shown in Fig. 3

Table 4 Result of water injection test by single loop methods in pit at the vadose zone

Lithology of investigated section	Location	Permeability (cm/s)	Average value (cm/s)	Classification of permeability
Clayey silt (qdl, eluvial soil)	North to the FPP	1.76×10^{-5}	3.40×10^{-5}	Aquitard
	West to the FPP	4.03×10^{-5}		
	South to the FPP	4.40×10^{-5}		

2016). In this study, groundwater and surface water during the wet, normal, and dry seasons were sampled in the field and analyzed in the laboratory. The single pollution index method is adapted to evaluate the contaminants in groundwater for all the analyzed factors (Wong et al. 2017):

$$S_i = \frac{C_i}{C_{si}} \tag{4}$$

where S_i is the contamination index of contaminant, C_i refers to the concentration of contaminant (unit mg/L for groundwater or quantity for the total coliform group), and C_{si} refers to the standard concentration of contaminant (unit mg/L for groundwater or quantity for the total coliform group). The standard of *quality standard for groundwater* (GB/T 14848–93) is employed for the evaluation: a value for S_i greater than 1 indicates that this type of contaminant is contaminated; in turn, it indicates that this contaminant meets the standard.

Results indicate that the groundwater at the site and in the local areas are of HCO_3–Ca, HCO_3^-, and SO_4–Ga types, and no significant contaminant in the groundwater is observed at the FPP and its vicinity. However, a few of the samples suffered contamination of coliform bacteria and ammonia nitrogen in both the wet and the dry seasons. Generally, the groundwater is less contaminated in the dry season than in the wet season, suggesting that it is more critical to protect the groundwater from being contaminated during the wet season (Table 5 and Fig. 3).

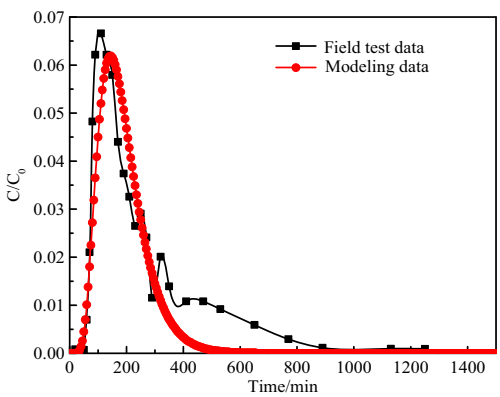

Fig. 6 Comparison of the field test and simulated concentrations of Na^+ ions

Risk assessment of groundwater contamination

Groundwater flow and transport modeling

Karst is a so extremely fragile natural environment that the delicate equilibrium of karst ecosystems can be dramatically and irreversibly changed as a consequence of both natural and anthropogenic impacts (Parise et al. 2015b). The issue concerning the migration of solute in the karst zone from the pollution source is an urgent and essential problem that should be addressed in groundwater assessment, taking into consideration the effect of the FPP itself on the hydrogeological regime. Based on the specific analysis of the geologic, hydrogeological, and geochemical characteristics of the site, a 2-D unconfined groundwater flow model was developed through the finite difference method using the MODFLOW code (McDonald and Harbaugh 1988). The equation governing contaminant transport through porous media can be derived from the principle of mass conservation. The advection-dispersion formula used for describing a solute transport is given by Zheng and Bennett (2002):

$$\nabla \cdot (\theta D \cdot \nabla c) - \nabla (qc) + q_s \cdot C_s = \theta \frac{\delta c}{\delta t} \tag{5}$$

where C is the contaminant concentration, D is the dispersion tensor, q is the volumetric water flux, θ is the volumetric water content, ∇ is the divergence operator, t is time, and q_s and C_s are the volumetric water flux and concentration of a contaminant sink/source term, respectively. No chemical reaction was considered in the model.

Contaminant transport parameters (e.g., retardation and dispersion) are known to be scale-dependent (Soltanian et al. 2017). In this case study, the model area extends approximately 5.01 km^2, demarcated by the rivers at the west-south-north of the site and the watershed to the east of the site. Infiltration of atmospheric precipitation dominates the recharge of groundwater in the model area, while rivers act as the destination for groundwater drainage. Generally, the effect of the anthropic intervention on the groundwater in the model area is negligible.

The conceptual model of the aquifer system was established based on the logs of more than 60 boreholes. The initial input parameters for the FPP and the ashery area are listed in Table 6. The infiltration coefficient of precipitation (α) and specific yield (μ) were fixed in 0.05 and 0.06,

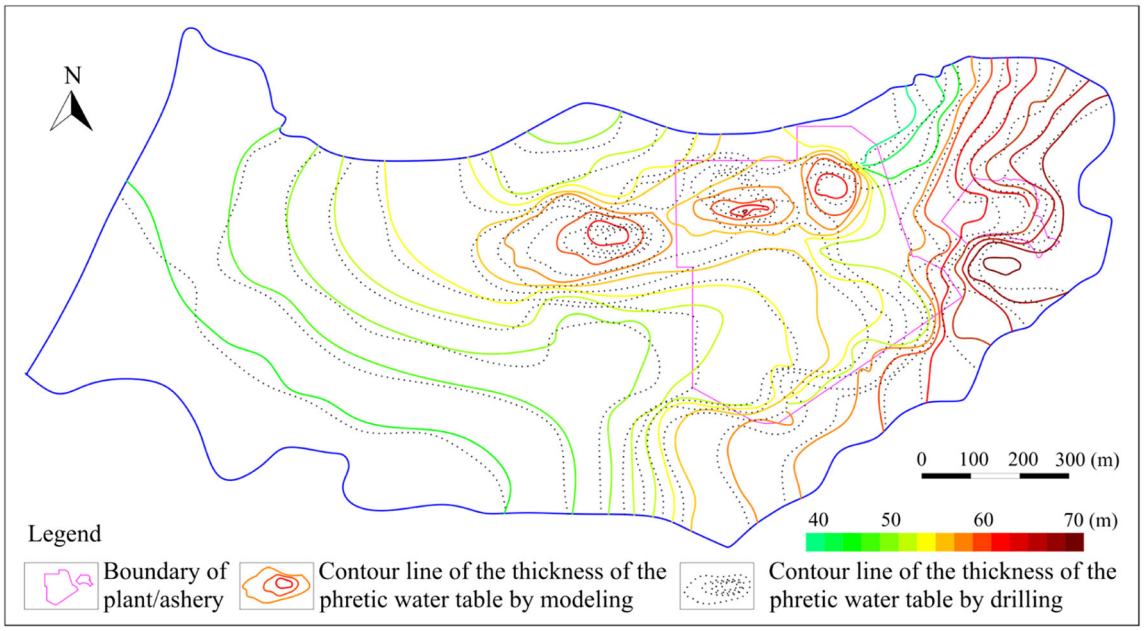

Fig. 7 Comparison of the contour map of between the measured and the calculated water table in the wet season

respectively, both for the region of the FPP and ashery. According to the tiny difference between the lithological characters of the FPP and ashery, the permeability (K) of the site at the FPP and ashery were set as 0.0173 and 0.013 m/day, respectively. Since little groundwater level data monitoring was performed in the area, the groundwater level measured in the

Table 5 Analysis results and evaluation of the present groundwater chemistry

Season		Dry season	Normal season	Wet season	Dry season	Normal season	Wet season	Dry season	Normal season	Wet season
Borehole no.	Item	Mn			Coliform bacteria (/L)			pH		
A	Ci	0.0011	0.0005	0.0008	–	3500	1700	6.91	7.17	7.09
	Si	0.011	0.005	0.008	–	*1166*	*566.67*	0.18	0.11	0.06
B	Ci	< 0.0001	0.0001	0.0007	–	230	9200	7.42	7.41	6.92
	Si	L	0.001	0.007	–	*76.67*	*3067*	0.28	0.27	0.16
C	Ci	0.16	0.0023	0.14	–	80	–	5.86	8.1	6.17
	Si	1.6	0.023	*1.4*	–	*26.66*	–	2.28	0.73	*1.66*
D	Ci	0.0001	0.0013	0.0008	–	16,000	230	7.76	7.28	7.48
	Si	0.001	0.013	0.008	–	*5333*	*76.67*	0.507	0.19	0.68
F	Ci	0.0013	0.0012	0.0005	–	9200	–	7.84	7.35	7.75
	Si	0.013	0.012	0.005	–	*3066*	–	0.56	0.23	0.5
G	Ci	0.0016	0.0004	0.0011	80	–	230	7.37	6.7	6.63
	Si	0.016	0.004	0.011	26.67	–	*76.67*	0.247	0.6	0.74
I	Ci	0.001	< 0.0001	0.0021	50	330	1700	7.36	8.1	6.97
	Si	0.01	–	0.021	16.67	*110*	*566.67*	0.24	0.73	0.06
J	Ci	0.0069	0.0005	0.0012	230	5400	5400	7.7	7.45	7.41
	Si	0.069	0.005	0.012	76.67	*1800*	*1800*	0.467	0.3	0.273
K	Ci	0.0045	0.0069	0.0007	130	490	700	7.59	7.9	7.45
	Si	0.045	0.069	0.007	43.33	*163.33*	*233.33*	0.393	0.6	0.3
Standard value		≤ 0.1			≤ 3.0			6.5–8.5		

Results for total hardness, sulfate, chloride, fluoride, nitrite nitrogen, nitrate nitrogen, iron, mercury, arsenic, cadmium, lead, hexavalent chromium, permanganate index, ammonia nitrogen, volatile phenol, and petroleum are below the standard value and not shown in the table. "-" indicates that the concentration in the sample is far less than the standard value. Italic numbers means that the concentration in the sample is beyond the standard value

Table 6 Initial value of hydrogeological parameters in the model

Region	Infiltration coefficient of precipitation/α	Permeability/ K (m/day)	Specific yield/μ	Lithological characters
FPP	0.05	0.0173	0.06	Pore water in friable rocks of quaternary, fissure-cavern water in carbonatite, fissure water in clastic rocks, and epimetamorphic rock
Ashery	0.05	0.013	0.06	

wet season during the investigation was used as the initial groundwater table in the model and was used for the model calibration. Figure 7 shows the comparison of contour maps between the computed and the measured groundwater table in the wet season. The calibrated groundwater flow model is quite consistent with the flow regime of the site, indicating the well-established validity of the model for further modeling of solute transport within the site. In other words, the current calibrated model is sufficient for the preliminary prediction of the groundwater behavior. Similar work of calibration and validation for groundwater flow model at site-local scale can be found in Yi et al. (2012a).

Plume transport and risk assessment

The transport behaviors of contaminant plumes preceded by accidental leaking were estimated based on the calibrated groundwater flow model. The aquifer system and the flow system were assumed to be the same for the solute transport model with those of the flow model. Scenarios with point contaminant sources have been hypothesized based on the layout of the FPP, including leaking at the diesel tank (DT), the industrial wastewater pool (IWP), the cooling tower water tank (CTWT), and the ashery. The point sources were estimated based on the design of the FPP and were listed in Table 7. The on-site tested longitudinal and transverse component of the dispersity, 0.033 m (α_L) and 0.009 m (α_T), were employed in the calculation. A total time of 30 years was calculated for the transport behavior of the plumes according to the operation period of the FPP.

For the FPP and the ashery under normal operating condition, the exhaust gas and wastewater produced during the operation will be environment-friendly treated and recycled by the established instruments before releasing to the environment. Therefore, no contaminants can reach the groundwater system and the risk is small for groundwater contamination.

However, the groundwater will be contaminated by accidental leaking at the FPP and plumes under normal operating condition. The transport distance and the distribution of the plumes at 100 days, 10 years, and 30 years are listed in Table 8. The distribution of the plumes after 30 years of transport from the DT, the IWP, and the CTWT are presented in Fig. 8. Results indicate that the maximum transport distances of contaminants released from DT, IWP, and CTWT are approximately 787, 363, and 769 m, respectively. Most of the plumes will be within the boundary of the FPP and the ashery. No contamination plume of petroleum, SO_4^{2-}, total dissolved solids (TDS), and Cl^- will reach the seven sensitive areas for occasional occurrence of groundwater pumping and usage. The shapes of contaminant plumes are distributed band-like in a direction from east to west, which can be attributed to the intertwined effect resulting from multiple factors including groundwater flow direction, intrinsic properties of diesel, the texture of the aquifers, and so on (Grima et al. 2015).

Based on the above prediction and analysis, it is clear that the construction and operation of the FPP and the ashery will present a limited risk for groundwater environmental contamination. Fortunately, the environmental protection objectives of this risk assessment are impervious to the contamination plumes that resulted from accidental leaking during the

Table 7 Scenarios for modeling of the accidental leaking and source calculations for the contaminates at the FPP

Item/location	Diesel storage tank piping	Industrial waste water pool			Water tank in cooling tower	
Leakage area (m^2)	0.0025	32			817.28	
Leakage rate per unit area (m/day)	3.2	1.39			35.55	
Leakage rate (m^3/day)	0.008	1.39			35.55	
Infiltration rate (m/day)	0.85	0.0435			0.0435	
Duration of leakage(days)	3	7300			7300	
Contaminant	Petroleum	Cl^-	TDS	SO_4^{2-}	SO_4^{2-}	TDS
Concentration (mg/L)	8×10^5	1500	2700	270	600	1300
Excessive concentration (mg/L)	0.05	250	450	250	250	450
Background concentration (mg/L)	–	10	130	10	10	130

Table 8 Results for the model prediction for accidental leaking at the diesel tank (DT), industrial wastewater pool (IWP), and cooling tower water tank (CTWT)

Source of pollution	Contaminant	Predictive time span	Area of pollution/m^2	Area of substandard/m^2	The max migration distance/m
Diesel tank (DT)	Diesel	100 days	14,315.18	13,814.91	102.1
		10 years	79,322.27	78,722.59	560.87
		30 years	92,858.67	92,158.35	786.97
Industrial wastewater pool (IWP)	Total salt (TS)	100 days	2996.4	2658.91	87.52
		10 years	19,264.46	18,639.46	197.04
		30 years	33,156.23	31,475.23	362.98
Cooling tower water tank (CTWT)	SO_4^{2-}	100 days	84,557.49	57,760.11	156.7
		10 years	133,478.01	119,194.53	330.32
		30 years	119,997.32	97,704.65	769.12

construction and operation period. Because of natural attenuation, both the transport distance and the distributed areas of the plumes will be slightly diminished despite a gigantic quantity of contaminated groundwater remaining. Herein, effective environmental measures should be taken for the construction and operation of the FPP and the ashery to avoid the occurrence of contamination.

Groundwater protection

Groundwater may deteriorate its quality and fail to be a renewable resource if not well managed because human intervention and natural processes change groundwater recharge patterns (Li et al. 2016b). To protect the soil and groundwater from being polluted, and to ensure the FPP under normal operation, effective environmental measures are needed. Priority is given to the grading of anti-seepage sites as well as the prevention and removal of the sources, given the inevitable leakage from potential pollution sources (Li et al. 2016a).

Results of the risk assessment and understanding of the site hydrogeology make it possible to program targeted anti-seepage measures by considering the layout of the FPP and the ashery. Three levels of anti-seepage have been proposed to prevent the groundwater from contamination: (1) the major control areas of 11.12 hm^2, including the oil reservoir region, the water tank in the cooling tower, and wastewater treatment of FPP and the ashery, which needs special anti-seepage layers with a hydraulic conductivity less than 10^{-12} cm/s; (2) the general control areas of the steam engine room, deaerator bay, and pump house, which are proposed to be constructed of concrete with a hydraulic conductivity less than 1.0×10^{-7} cm/s; and (3) The minor control areas of administrative office, transformer substation, canteen, and so on, which the standard concrete measure is proposed for anti-seepage purposes.

In the meantime, a total of 11 wells have been designated for monitoring the groundwater system and for the protection of the sensitive areas involving groundwater usage. The monitoring wells are designated according to the following

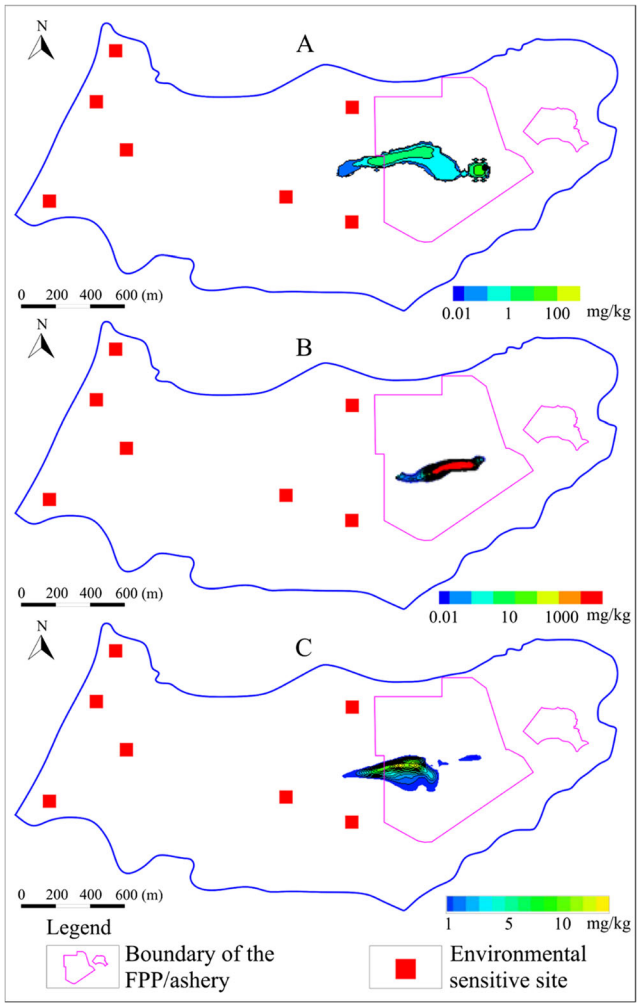

Fig. 8 Distribution of the contamination plume after 30 years of transport preceded by accidental leaking: **a** diesel plume from the diesel tank (DT), **b** total dissolved solids (TDS) plume from the industrial wastewater pool (IWP), and **c** sulfate radical plume from the cooling tower water tank (CTWT)

requirements: (1) enhanced monitoring in major pollution control regions and adjust locally by the position of pollution sources as well as the groundwater flow direction; (2) primary focus on the shallow aquifers; (3) taking into account groundwater monitoring in the vicinity of the FPP and the ashery; (4) monitoring both the upstream background, the lateral condition of the FPP, and the sensitive downstream areas; and (5) monitoring both the groundwater level and the chemistry. The distribution of the monitoring wells is shown in Fig. 3.

Conclusion

A risk assessment of groundwater environmental contamination is presented for the construction of FPP at a karst site with limited prior knowledge. This case study illustrated the assessment procedure, contents, and the relationship between the groundwater system and the project characteristics of the FPP, focusing mainly on the hydrogeological characteristics of the site through an integrated on-site surface, subsurface, and laboratory investigations supplemented by solute transport modeling. Results indicate that the site is located in a synclinal basin area and represents a semi-isolated hydrogeological unit with groundwater discharge to the Beijiang River along the western boundary. The vadose zone presents poor permeability and acts as a horizontal cutoff wall to restrict the infiltration of contaminants through the vadose zone to the subsurface. The aquifers consist of the filled karst development area with a thickness ranging from 6.0 to 40.0 m, which mainly distributed in the middle-south part of the site. No shallow buried river, hall- or corridor-type karst caves were developed at the site, nor large-scale well-connectivity karst channels. Karstified carbonates framework were found to be filled with silt clay, revealing the hydrogeological system is hydraulic continuous and inactive, which premised the correct interpretation and modeling of solute transport. Groundwater flows mainly from the east to the west with annual fluctuation around 0.2 to 4.0 m. The groundwater partly suffers contamination from *coliform* bacteria and ammonia nitrogen.

Seven decentralized domestic well areas are confirmed as environmentally sensitive areas after the detailed investigation on the pollution sources and monitoring. Results of numerical modeling and prediction indicate that the groundwater will be partly contaminated with a certain period at the point source area of the FPP. The maximum transport distances of contaminants released from DT, IWP, and CTWT are approximately 787, 363, and 769 m, respectively. Most of the plumes will be within the boundary of the FPP and the ashery. No contamination plume of petroleum, SO_4^{2-}, TDS, and Cl^- will reach the seven sensitive areas. A suggested course for anti-seepage measures and monitoring was proposed for the protection of the groundwater based on the results of the risk assessment. This study provides a valid integrated approach for investigation and risk assessment of groundwater contamination for a construction project and is most valuable for the purposes of site selection, project design, and protection of the groundwater environment.

Acknowledgements This work was supported by Shenzhen Municipal Science and Technology Innovation Committee through project Shenzhen Key Laboratory of Soil and Groundwater Pollution Control (No. ZDSY20150831141712549) and Shenzhen fundamental research project (JCYJ20150831142213741). Partial funding has also been supported by Shenzhen Peacock Plan (No. KQTD2016022619584022).

References

Anand RR, Aspandiar MF, Noble RRP (2016) A review of metal transfer mechanisms through transported cover with emphasis on the vadose zone within the Australian regolith. Ore Geol Rev 73:394–416. https://doi.org/10.1016/j.oregeorev.2015.06.018

Arias-Estévez M, López-Periago E, Martínez-Carballo E, Simal-Gándara J, Mejuto J-C, García-Río L (2008) The mobility and degradation of pesticides in soils and the pollution of groundwater resources. Agric Ecosyst Environ 123(4):247–260. https://doi.org/10.1016/j.agee.2007.07.011

Calò F, Parise M (2009) Waste management and problems of groundwater pollution in karst environments in the context of a post-conflict scenario: the case of Mostar (Bosnia Herzegovina). Habitat Int 33(1):63–72. https://doi.org/10.1016/j.habitatint.2008.05.001

Chandra S, Saxena T, Nehra S, Mohan MK (2016) Quality assessment of supplied drinking water in Jaipur city, India, using PCR-based approach. Environ Earth Sci 75(2):153. https://doi.org/10.1007/s12665-015-4809-5

Dai Z, Samper J (2004) Inverse problem of multicomponent reactive chemical transport in porous media: formulation and applications. Water Resour Res 40:294–295. https://doi.org/10.1029/2004WR003248

Ducci D, Masi GD, Priscoli GD (2008) Contamination risk of the Alburni karst system (southern Italy). Eng Geol 99(3-4):109–120. https://doi.org/10.1016/j.enggeo.2007.11.008

Feinstein DT, Guo W (2004) STANMOD: a suite of windows-based programs for evaluating solute transport. Groundwater 42(4):482–487. https://doi.org/10.1111/j.1745-6584.2004.tb02615.x

Fernández-Cruz T, Martínez-Carballo E, Simal-Gándara J (2017) Perspective on pre- and post-natal agro-food exposure to persistent organic pollutants and their effects on quality of life. Environ Int 100:79–101. https://doi.org/10.1016/j.envint.2017.01.001

Ford D, Williams PW (2007) Karst hydrogeology and geomorphology. Karst hydrogeology and geomorphology. Wiley. https://doi.org/10.1002/9781118684986

Goss MJ, Ehlers W, Unc A (2010) The role of lysimeters in the development of our understanding of processes in the vadose zone relevant to contamination of groundwater aquifers. Phys Chem Earth 35(15-18):913–926. https://doi.org/10.1016/j.pce.2010.06.004

Grima J, Luque-Espinar JA, Mejía JA, Rodríguez R (2015) Methodological approach for the analysis of groundwater quality in the framework of the groundwater directive. Environ Earth Sci 74:1–13. https://doi.org/10.1007/s12665-015-4472-x

Gurdak JJ, Qi SL (2012) Vulnerability of recently recharged groundwater in principal [corrected] aquifers of the United States to nitrate contamination. Environ Sci Technol 46(11):6004–6012. https://doi.org/10.1021/es300688b

Gutiérrez F, Parise M, Waele JD, Jourde H (2014) A review on natural and human-induced geohazards and impacts in karst. Earth Sci Rev 138:61–88. https://doi.org/10.1016/j.earscirev.2014.08.002

Idris AN, Aris AZ, Praveena SM, Suratman S, Tawnie I, Samsuddin MKN, Sefei A (2016) Hydrogeochemistry characteristics in Kampong Salang, Tioman Island, Pahang, Malaysia. Materials Science and Engineering Conference Series, pp 012065. https://doi.org/10.1088/1757-899X/136/1/012065

Kaufmann G, Braun J (1999) Karst aquifer evolution in fractured, porous rocks. J Hydrol 35:3223–3238. https://doi.org/10.1016/j.jhydrol.2016.10.049

Khaleel R (2007) Impact assessment of existing vadose zone contamination at the Hanford site SX tank farm. Vadose Zone J 6(4):935–945. https://doi.org/10.2136/vzj2006.0176

Lacey R (2016) The characteristic flow equation: a tool for engineers and scientists. Geotext Geomembr 44(4):534–548. https://doi.org/10.1016/j.geotexmem.2016.03.001

Li J, Li X, Lv N, Yang Y, Xi B, Li M, Bai S, Liu D (2015) Quantitative assessment of groundwater pollution intensity on typical contaminated sites in China using grey relational analysis and numerical simulation. Environ Earth Sci 74(5):3955–3968. https://doi.org/10.1007/s12665-014-3980-4

Li J, Yang Y, Huan H, Li M, Xi B, Lv N, Wu Y, Xie Y, Li X, Yang J (2016a) Method for screening prevention and control measures and technologies based on groundwater pollution intensity assessment. Sci Total Environ 551-552:143–154. https://doi.org/10.1016/j.scitotenv.2015.12.152

Li P, Li X, Meng X, Li M, Zhang Y (2016b) Appraising groundwater quality and health risks from contamination in a semiarid region of Northwest China. Exposure and Health 8(3):361-379. https://doi.org/10.1007/s12403-016-0205-y

Li P, Tian R, Xue C, Wu J (2017) Progress, opportunities, and key fields for groundwater quality research under the impacts of human activities in China with a special focus on western China. Environ Sci Pollut Res 24(15):13224–13234. https://doi.org/10.1007/s11356-017-8753-7

Marín AI, Andreo B, Mudarra M (2010) Importance of evaluating karst features in contamination vulnerability and groundwater protection assessment of carbonate aquifers. The case study of Alta Cadena (southern Spain). Z Geomorphol 54(2):179–194(16). https://doi.org/10.1127/0372-8854/2010/0054S2-0010

Mayer AS, Kelley CT, Miller CT (2002) Optimal design for problems involving flow and transport phenomena in saturated subsurface systems. Adv Water Resour 25(8-12):1233–1256. https://doi.org/10.1016/S0309-1708(02)00054-4

McDonald MG, Harbaugh AW (1988) A modular three-dimensional finite-difference ground-water flow model. United States: Department of the Interior, Reston, VA (US). https://doi.org/10.1016/0022-1694(86)90106-X

Mejías M, Renard P, Glenz D (2009) Hydraulic testing of low-permeability formations: a case study in the granite of Cadalso de los Vidrios, Spain. Eng Geol 107(3-4):88–97. https://doi.org/10.1016/j.enggeo.2009.05.010

Parise M, Closson D, Gutiérrez F, Stevanović Z (2015a) Anticipating and managing engineering problems in the complex karst environment. Environ Earth Sci 74(12):7823–7835. https://doi.org/10.1007/s12665-015-4647-5

Parise M, Ravbar N, Živanović V, Mikszewski A, Kresic N, Mádl-Szőnyi J, Kukurić N (2015b) Hazards in karst and managing water resources quality, karst aquifers—characterization and engineering. Springer, pp 601–687. https://doi.org/10.1007/978-3-319-12850-4_17

Pfunt H, Houben G, Himmelsbach T (2016) Numerical modeling of fracking fluid migration through fault zones and fractures in the north German Basin. Hydrogeol J 24:1–16. https://doi.org/10.1007/s10040-016-1418-7

Samper J, Yang C, Zheng L, Montenegro L, Xu T, Dai Z, Zhang G, Lu C, S. M. (2012) CORE2D V4: A code for water flow, heat and solute transport, geochemical reactions, and microbial processes. In: Zhang F, Yeh G-T, and Parker JC (eds) Groundwater Reactive Transport Models. Bentham Open E-Books, pp 160–185. https://doi.org/10.1007/s10040-016-1464-1

Shan M, Zhang S (2012) Research and practice on interface management in large-scale industrial construction project. Appl Mech Mater 174-177:3387–3392. https://doi.org/10.4028/www.scientific.net/AMM.174-177.3387

Soltanian MR, Sun A, Dai Z (2017) Reactive transport in the complex heterogeneous alluvial aquifer of Fortymile Wash, Nevada. Chemosphere 179:379–386. https://doi.org/10.1016/j.chemosphere.2017.03.136

Stuart M, Lapworth D, Crane E, Hart A (2012) Review of risk from potential emerging contaminants in UK groundwater. Sci Total Environ 416:1–21. https://doi.org/10.1016/j.scitotenv.2011.11.072

Wachniew P, Zurek AJ, Stumpp C, Gemitzi A, Gargini A, Filippini M, Rozanski K, Meeks J, Kvaerner J, Witczak S (2016) Towards operational methods for the assessment of intrinsic groundwater vulnerability: a review. Critical Reviews in Environmental Sciences and Technology (9), 00-00. https://doi.org/10.1080/10643389.2016.1160816

Waltham AC, Fookes PG (2011) Engineering classification of karst ground conditions. Q J Eng Geol Hydrogeol 36:101–118. https://doi.org/10.1144/1470-9236/2002-33

Wong KW, Yap CK, Nulit R, Hamzah MS, Chen SK, Wan HC, Karami A, Al-Shami SA (2017) Effects of anthropogenic activities on the heavy metal levels in the clams and sediments in a tropical river. Environ Sci Pollut Res 24(1):116–134. https://doi.org/10.1007/s11356-016-7951-z

Worthington S, Ford D, Beddows P (2001) Characteristics of porosity and permeability enhancement in unconfined carbonate aquifers due to the development of dissolutional channel systems. Present state and future trends of karst studies. UNESCO, 1, 13-29

Yeh WW-G (2015) Review: optimization methods for groundwater modeling and management. Hydrogeol J 23(6):1051–1065. https://doi.org/10.1007/s10040-015-1260-3

Yi SP, Ma H, Wang H (2012a) A preliminary study on the transport behavior for a potential disposal site of LILW in southern china. Progress in environmental science and engineering (Iceesd 2011), Pts 1-5, 356-360, 1445-1453. https://doi.org/10.4028/www.scientific.net/AMR.356-360.1445

Yi S, Samper J, Naves A, Soler JM (2012b) Identifiability of diffusion and retention parameters of anionic tracers from the diffusion and retention (DR) experiment. J Hydrol Sci 446-447:70-76. https://doi.org/10.1016/j.jhydrol.2012.04.032

Zech A, Arnold S, Schneider C, Attinger S (2015) Estimating parameters of aquifer heterogeneity using pumping tests—implications for field applications. Adv Water Resour 83:137–147. https://doi.org/10.1016/j.advwatres.2015.05.021

Zhang B, Li G, Cheng P, Yeh TCJ, Hong M (2016) Landfill risk assessment on groundwater based on vulnerability and pollution index. Water Resour Manag 30(4):1465–1480. https://doi.org/10.1007/s11269-016-1233-x

Zheng C, Bennett GD (2002) Applied contaminant transport modeling, 2. Wiley-Interscience, New York